

Thresholded Multivariate Principal Component Analysis for Multi-channel Profile Monitoring

Yuan Wang, Kamran Paynabar, Yajun Mei

H. Milton Stewart School of Industrial and Systems Engineering, Georgia Institute of Technology

February 28, 2022

Abstract

Monitoring multichannel profiles has important applications in manufacturing systems improvement, but it is non-trivial to develop efficient statistical methods due to two main challenges. First, profiles are high-dimensional functional data with intrinsic inner- and inter-channel correlations, and one needs to develop a dimension reduction method that can deal with such intricate correlations for the purpose of effective monitoring. The second, and probably more fundamental, challenge is that the functional structure of multi-channel profiles might change over time, and thus the dimension reduction method should be able to automatically take into account the potential unknown change. To tackle these two challenges, we propose a novel thresholded multivariate principal component analysis (PCA) method for multi-channel profile monitoring. Our proposed method consists of two steps of dimension reduction: It first applies the functional PCA to extract a reasonable large number of features under the normal operational (in-control) state, and then use the soft-thresholding techniques to further select significant features capturing profile information in the out-of-control state. The choice of tuning parameter for soft-thresholding is provided based on asymptotic analysis, and extensive simulation studies are conducted to illustrate the efficacy of our proposed thresholded PCA methodology.

Keywords: Thresholding Estimation, Principal Component Analysis, Multichannel Profiles, Nonlinear Profiles, Phase I monitoring, Statistical Process Control (SPC).

1 Introduction

Profile monitoring plays an important role in manufacturing systems improvement (Noorossana et al. (2011), Qiu (2013)), and a standard setup is to monitor a sequence of profiles (e.g. curves or functions) over time to check whether the underlying functional structure of the profiles changes or not. Extensive research has been done for monitoring *univariate* profile or *real-valued* functions in the area of statistical process control (SPC) in the past decades, and standard approaches are to reduce the univariate profiles in the infinite-dimensional or high-dimensional functional spaces to a low-dimensional set of features (e.g., shape, magnitude, frequency, regression coefficients, etc.). See, for instance, work by Jin and Shi (2000), Ding et al. (2006), Jeong et al. (2006), Jensen et al. (2008), Berkes et al. (2009), Chicken et al. (2009), Qiu et al. (2010), Abdel-Salam et al. (2013).

Nowadays manufacturing systems are often equipped with a variety of sensors capable of collecting several profile data simultaneously, and thus one often faces the problem of monitoring multichannel or multivariate profiles that have rich information about systems performance. A concrete motivating example of this paper is from a forging process, shown in Figure 1 and 2, in which multichannel load profiles measure exerted forces in each column of the forging machine. Here each data is a four-dimensional vector function or four curves that have similar but not identical shapes when the machine is operating under the normal state. While various methods have been developed for univariate profile monitoring, they often cannot easily be extended to multichannel profiles, and research on monitoring multivariate/multichannel nonlinear profiles is very limited. For some exceptions, see Jeong et al. (2007), Paynabar et al. (2013), Grasso et al. (2014), and Paynabar et al. (2016). There are two main challenges when monitoring multichannel profiles. The first one is that profiles are high-dimensional functions with intrinsic inner- and inter-channel correlations, and one needs to develop a dimension reduction method that can deal with such intricate correla-

tions. The second, probably more fundamental, challenge is that the functional structure of multi-channel profiles might change over time, and thus the dimension reduction method should be able to take into account the potential unknown change.

The primary goal of this paper is to develop an effective statistical method for monitoring multichannel profiles. Our methodology is inspired by the functional Principal Component Analysis (PCA), which has been successfully applied by Paynabar et al. (2013), Grasso et al. (2014), and Paynabar et al. (2016) to deal with intrinsic inner- and inter-channel correlations of profiles. These existing methods follow the standard PCA approach to select a few principal components (projections or eigenvectors) that contain a large amount of variation or information in the profile data under the normal operational (in-control) state. This kind of dimension reduction approach might be reasonable from the estimation or curve fitting/smoothing viewpoint under the normal operation state, but unfortunately it is ineffective in the context of process monitoring, especially for multivariate or multi-channel profiles. This is because it does not reflect the possible change or fail to capture the profile information under the out-of-control state. Here we propose to develop a PCA method that can automatically take into account the potential unknown change.

Note that there are two different phases of profile monitoring: one is Phase I for offline analysis when a retrospective data set is used to estimate and refine the underlying model and its parameters, and the other is Phase II when the estimated model in Phase I is used for online process monitoring. Here we focus on the Phase I analysis, and hopefully our results can shed new light for Phase II monitoring of multichannel profiles as well. In addition, we should acknowledge that the importance of dimension reduction and feature selection for high-dimensional data via thresholding or shrinkage is well-known in modern statistics, including the profile monitoring literature. Jeong et al. (2006) incorporated the hard thresholding into the Hotelling T^2 statistics in the context of online monitoring of single profiles, and Jeong et al. (2007) proposed a hard thresholding method to obtain

projection information by optimizing “overall relative reconstruction error”. Zou et al. (2012) applied LASSO shrinkage in linear model coefficients for online monitoring linear profiles problem. However, these existing methods use thresholding or shrinkage to conduct *one-shot* dimension reduction, whereas our proposed methodology splits the dimension reduction process into two steps using two different methods: PCA for the normal operation or in-control state, and soft-thresholding for the out-of-control state.

The remainder of this paper is organized as follows. In Section 2, we present the mathematical formulation of multichannel profile monitoring. In Section 3, we propose our thresholded PCA method, and provide a guideline on how to select the corresponding tuning parameters. In Section 4, we use the real forging process data and simulations to illustrate the usefulness of our proposed thresholded PCA method. Concluding remarks and future research directions are presented in Section 5.

2 Problem Formulation and Background

Suppose that a random sample of m multichannel profiles, each with p channels, is collected from a production process. Mathematically, each of the m multichannel profile observations is a p -dimensional curve denoted by $\mathbf{X}_i(t) = (X_i^{(1)}(t), \dots, X_i^{(p)}(t))^T$, where $t \in [0, 1]$, for $i = 1, \dots, m$. We assume that the process is initially in-control and at some unknown time τ , the process may become out-of-control in the sense of the mean shifts of the profiles $\mathbf{X}_i(t)$ ’s. Specifically, we assume that the data are from the change-point additive noise model

$$\mathbf{X}_i(t) = \begin{cases} \boldsymbol{\mu}_1(t) + \mathbf{Y}_i(t), & \text{when } i = 1, \dots, \tau, \\ \boldsymbol{\mu}_2(t) + \mathbf{Y}_i(t), & \text{when } i = \tau + 1, \dots, m, \end{cases} \quad \text{for } 0 \leq t \leq 1, \quad (1)$$

for some unknown $0 \leq \tau < m$, where the $\mathbf{Y}_i(t)$ ’s are independent and identically distributed (i.i.d.) p -dimensional “noise” curves with mean $\mathbf{0}$, i.e., $\mathbf{Y}_i(t) = (\mathbf{Y}_i^{(1)}(t), \dots, \mathbf{Y}_i^{(p)}(t))^T$ and

$\mathbf{E}(\mathbf{Y}_i^{(j)}(t)) = 0$ for all dimension $j = 1, \dots, p$ and for all observations $i = 1, \dots, m$.

In Phase I profile monitoring, $\boldsymbol{\mu}_1(t)$ and $\boldsymbol{\mu}_2(t)$ are two unknown p -dimensional mean functions, and we want to utilize the observed $\mathbf{X}_i(t)$'s to test the null hypothesis $H_0 : \boldsymbol{\mu}_1(t) = \boldsymbol{\mu}_2(t)$ (i.e., no change) against the alternative hypothesis $H_a : \boldsymbol{\mu}_1(t) \neq \boldsymbol{\mu}_2(t)$ (i.e., a change occurs at some unknown time $0 \leq \tau < m$). In addition, we also impose the classical Type I probability error constraint $P_{H_0}(\text{reject } H_0 : \boldsymbol{\mu}_1(t) = \boldsymbol{\mu}_2(t)) \leq \alpha$, for some pre-specified constant α , e.g., $\alpha = 5\%$.

To test the hypothesis $H_0 : \boldsymbol{\mu}_1(t) = \boldsymbol{\mu}_2(t)$ under model (1) subject to the Type I error constraint, it is important to make suitable assumptions of the correlation of both within and between profile channels. To characterize these correlations, as in Paynabar et al. (2016), we apply Karhunen-Loeve expansion theorem to the p -dimensional noise curves $\mathbf{Y}_i(t)$: there exists a set of orthonormal (orthogonal and unit norm) basis functions $\mathcal{V} = \{v_k(t) \in L_2[0, 1], k = 1, 2, \dots\}$, such that

$$\mathbf{Y}_i(t) = \sum_{k \in \mathcal{V}} \boldsymbol{\xi}_{ik} v_k(t), \quad \text{for } i = 1, \dots, m, \quad (2)$$

where the number of elements of \mathcal{V} could be either finite or infinite, and the coefficient $\boldsymbol{\xi}_{ik} = (\xi_{ik1}, \dots, \xi_{ikp})$ is a p -dimensional vector. The key assumption we made is that the coefficients $\{\boldsymbol{\xi}_{ik}\}$'s are i.i.d. p -dimensional random vectors with mean $\mathbf{0}$ and covariance matrix Σ_k over all $i = 1, \dots, m$ data points for each base $k \in \mathcal{V}$. Under this assumption, it is evident from (2) that the $p \times p$ covariance matrix Σ_k satisfies

$$\Sigma_k = \mathbf{E}(\boldsymbol{\xi}_{ik} \boldsymbol{\xi}_{ik}^T) = \mathbf{E}\left\{\int_0^1 \mathbf{Y}_i(t) v_k(t) dt \int_0^1 \mathbf{Y}_i(t)^T v_k(t) dt\right\}, \quad (3)$$

since the basis functions $v_k(t)$'s are orthonormal for each $k \in \mathcal{V}$.

It is useful to briefly discuss the effect of (2) on the correlations of multichannel profiles. As in the standard functional data analysis, the real-valued basis functions $v_k(t)$'s are closely related to the *inner-channel* correlation of the profiles. Meanwhile, since the p -dimensional

curve is decomposed into the same real-valued basis functions $v_k(t)$'s in (2), the *inter-channel* correlations of the p -channel profiles are characterized by the correlation matrices Σ_k 's in (3) of the coefficients $\{\boldsymbol{\xi}_{ik}\}$'s. In practice, both the basis functions $v_k(t)$'s and the covariance matrices Σ_k 's are unknown and needed to be estimated, see the next section.

3 Our Proposed Thresholded PCA Methodology

In this section, we develop a thresholded multivariate functional PCA methodology for Phase I monitoring of multichannel profiles. For the purpose of easy understanding, this section is subdivided into three subsections. In Subsection 3.1, we review the multivariate functional PCA method that estimates the basis $v_k(t)$'s in (2) and the covariance matrices Σ_k 's in (3). This allows us to reduce the data from the space of p -dimensional profiles $\mathbf{X}_i(t)$'s to the space of the coefficients $\boldsymbol{\xi}_{ik}$'s in (2) under the normal operational or in-control state. In Subsection 3.2, our proposed method is developed as a hypothesis test for the change-point model in (1) augmented by soft-thresholding technique that has a nature semi-Bayesian interpretation and is closely related to the generalized likelihood ratio test. Here the soft-thresholding selects significant coefficients $\boldsymbol{\xi}_{ik}$'s in (2) that are likely affected by the change, and thus can be thought of as a further dimension reduction under the out-of-control state. In Subsection 3.3, based on asymptotic analysis, we provide a guidance on the choice of tuning parameters in our proposed thresholded PCA methodology.

3.1 Basis and Covariance Estimation

To have a better understanding of the basis and covariance matrix estimation under the change-point model in (1), we first consider the estimation under the unrealistic case when the noise functions $\mathbf{Y}_i(t)$'s in (2) were observable. Recall that the p -dimensional functions $\mathbf{Y}_i(t)$'s are decomposed into the same real-valued basis functions $v_k(t)$'s in (2), this mo-

tivates us to evaluate the *inner-channel* correlation of $\mathbf{Y}_i(t)$'s by the following covariance function:

$$c(t, s) = \mathbf{Cov}\{\mathbf{Y}_i(t), \mathbf{Y}_i(s)\} = \sum_{j=1}^p \mathbf{E}(Y_i^{(j)}(t) \cdot Y_i^{(j)}(s)) \quad \text{for } 0 \leq t, s \leq 1, \quad (4)$$

since $\mathbf{Y}_i(t)$ is a p -dimensional function with mean $\mathbf{0}$. When $p = 1$, the covariance function $c(t, s)$ in (4) is well studied, and it is well-known that the bases $v_k(t)$'s are the eigenfunctions of $c(t, s)$. Below we will show that similar conclusions also hold under our definition of the covariance function $c(t, s)$ in (4) for the general $p \geq 2$ case.

To see this, since the basis functions $v_k(t)$'s are orthonormal, it follows from (2) that $c(t, s) = \sum_{k=1}^{\infty} \sum_{j=1}^p \mathbf{E}[\xi_{ikj}^2] v_k(t) v_k(s)$, and $\int_0^1 c(t, s) v_k(s) ds = \lambda_k v_k(t)$, where $\lambda_k = \sum_{j=1}^p \mathbf{E}[\xi_{ikj}^2]$, and ξ_{ikj} is the j -th component of the p -dimensional random vector $\boldsymbol{\xi}_{ik}$ for $j = 1, \dots, p$. Hence, the basis $v_k(t)$'s are the eigenfunctions of $c(t, s)$ for any dimension $p \geq 2$.

It suffices to estimate the covariance function $c(t, s)$ in (4) from the observable profiles $\mathbf{X}_i(t)$. While the noise terms $\mathbf{Y}_i(t)$'s are unobservable, a good news of the change-point additive noise model in (1) is that the differences $\mathbf{Y}_{i+1}(t) - \mathbf{Y}_i(t) = \mathbf{X}_{i+1}(t) - \mathbf{X}_i(t)$ are observable for all $1 \leq i \leq m-1$ except $i = \tau$ (the change-point). Thus the covariance function $c(t, s)$ in (4) can be estimated by $\mathbf{Y}_{i+1}(t) - \mathbf{Y}_i(t)$, which yields the approximation:

$$\hat{c}(t, s) = \frac{1}{2(m-1)} \sum_{i=1}^{m-1} (\mathbf{X}_{i+1}(t) - \mathbf{X}_i(t))^T (\mathbf{X}_{i+1}(s) - \mathbf{X}_i(s)). \quad (5)$$

Note that the denominator is $2(m-1)$, and since the $\mathbf{Y}_i(t)$'s are i.i.d. over $i = 1, \dots, m$, the estimated function $\hat{c}(t, s)$ in (5) is consistent under the reasonable regularity assumption of the alternative hypothesis, see Remark #2 in Paynabar et al. (2016).

Next, the estimates of basis functions $\hat{v}_k(t)$'s can be found as the eigenfunctions of $\hat{c}(t, s)$ in (5). As for the estimation of the covariance matrix Σ_k in (3) of coefficients $\boldsymbol{\xi}_{ik}$, we again take advantage of the differences $\mathbf{Y}_{i+1}(t) - \mathbf{Y}_i(t)$ under the change-point additive noise

model in (1), and approximate it by

$$\hat{\Sigma}_k = \frac{1}{2(m-1)} \sum_{i=1}^{m-1} \int_0^1 \{\mathbf{X}_{i+1}(t) - \mathbf{X}_i(t)\} \hat{v}_k(t) dt \int_0^1 \{\mathbf{X}_{i+1}(t) - \mathbf{X}_i(t)\}^T \hat{v}_k(t) dt. \quad (6)$$

We follow the standard PCA literature to focus on the first d largest eigenvalues of the function $\hat{c}(t, s)$ in (5), and consider the corresponding d eigenfunctions $\hat{v}_k(t)$'s. However, our choice of the actual value of d will be different here. From the dimension reduction viewpoint, the standard PCA methods often reduce the data directly to a low-dimensional space, and thus the value of d is often chosen to be relatively small. Meanwhile, for our proposed method, the dimension reduction process is split into two steps that correspond to the normal operation state and the out-of-control state, respectively. The PCA is used only in the first step to reduce the data from the infinitely functional (or super-high-dimensional) space to an intermediate space of R^d , which will be further reduced to a lower-dimensional space in the second step. As a result, the number d of the chosen principal components of the PCA can be moderately large for our proposed method, e.g., fifties or hundreds.

3.2 Thresholded PCA for Monitoring

We are ready to present our proposed method that utilizes the observed profiles $\mathbf{X}_i(t)$'s to test $H_0 : \boldsymbol{\mu}_1(t) = \boldsymbol{\mu}_2(t)$ under the change-point additive noise model (1). Intuitively, it is natural to construct a test statistic based on the estimation of $\boldsymbol{\mu}_1(t) - \boldsymbol{\mu}_2(t)$. This suggests us to compare the difference of profile sample means before and after a potential change-point $\ell = 1, 2, \dots, m-1$,

$$\Delta_\ell(t) = \sqrt{\frac{\ell(m-\ell)}{m}} \left\{ \frac{1}{\ell} \sum_{i=1}^{\ell} \mathbf{X}_i(t) - \frac{1}{m-\ell} \sum_{i=\ell+1}^m \mathbf{X}_i(t) \right\}. \quad (7)$$

Here the term $\sqrt{\ell(m-\ell)/m}$ scales the difference and standardizes the variance of profile difference. Note that the function $\Delta_\ell(t)$ in (7) would have mean $\mathbf{0}$ when $H_0 : \boldsymbol{\mu}_1(t) = \boldsymbol{\mu}_2(t)$ is true, but have non-zero mean under $H_a : \boldsymbol{\mu}_1(t) \neq \boldsymbol{\mu}_2(t)$ when $\ell = \tau$ (the change-point).

Next, with the estimated orthonormal basis $\hat{v}_k(t)$'s and estimated covariance matrix $\hat{\Sigma}_k$ in (6), we apply the PCA decomposition in (2) to the function $\Delta_\ell(t)$ in (7). This essentially projects the test statistics from the functional space to a d -dimensional space under the normal operational or in-control state. Specifically, for each candidate change-point $\ell = 1, 2, \dots, m-1$, define the projection to each of the first d principal components, $\boldsymbol{\eta}_{\ell k} = \int_0^1 \Delta_\ell(t) \hat{v}_k(t) dt$, and then compute the corresponding real-valued statistic

$$U_{\ell,k} = \boldsymbol{\eta}_{\ell k}^T \hat{\Sigma}_k^{-1} \boldsymbol{\eta}_{\ell k} \quad (8)$$

for $k = 1, 2, \dots, d$, where $\hat{\Sigma}_k$ is defined in (6).

Note that the statistics $U_{\ell,k}$'s in (8) are motivated from the scenario when the basis $\nu_k(t)$ and Σ_k are known: if the estimates $\hat{v}_k(t)$ and $\hat{\Sigma}_k$ are replaced by their true values, it is straightforward from (1) to show that $\boldsymbol{\eta}_{\ell k} \sim N(\mathbf{0}, \Sigma_k)$ under the null hypothesis $H_0 : \boldsymbol{\mu}_1(t) = \boldsymbol{\mu}_2(t)$ but $\boldsymbol{\eta}_{\ell k} \sim N(\int_0^1 \Delta_\ell(t) \nu_k(t) dt, \Sigma_k)$ under the alternative hypothesis $H_a : \boldsymbol{\mu}_1(t) \neq \boldsymbol{\mu}_2(t)$. Hence, when the basis $\nu_k(t)$ and Σ_k are known, the $U_{\ell,k}$'s in (8) are χ_p^2 -distributed under H_0 but should be stochastically larger than χ_p^2 under H_a . When the estimates $\hat{v}_k(t)$ and $\hat{\Sigma}_k$ are used, we expect that similar conclusions also hold approximately, e.g., whether the value of $U_{\ell,k}$ in (8) is large or small indicates whether there is a change along the principal component $\hat{v}_k(t)$ or not.

Finally, our proposed thresholded PCA methodology considers the soft-thresholding transformation of the $U_{\ell,k}$'s in (8), so as to smooth out those noisy principal component $\hat{v}_k(t)$'s that do not provide information about the change under the out-of-control state. To be more rigorous, we propose a test statistic defined by

$$Q_m = \max_{1 \leq \ell < m} \sum_{k=1}^d (U_{\ell,k} - c)^+, \quad (9)$$

for some pre-specified ‘‘soft-thresholding’’ parameter $c \geq 0$. Here $(u - c)^+ = \max(u - c, 0)$.

Then we reject the null hypothesis $H_0 : \boldsymbol{\mu}_1(t) = \boldsymbol{\mu}_2(t)$ if and only if

$$Q_m > L \quad (10)$$

for some pre-determined threshold L . The choices of the constants c and L will be discussed in more detail in the next section. When $Q_m > L$, we not only claim that there exists a change point, but also can estimate the change point by

$$\hat{\tau} = \arg \max_{1 \leq \ell < m} \sum_{k=1}^d (U_{\ell,k} - c)^+. \quad (11)$$

It is informative to provide some high-level insights of the test statistic Q_m in (9). Since we do not know the true change-point τ , it is natural to maximize (9) over all candidate change-points $\tau = \ell$ for $1 \leq \ell < m$ from the maximum likelihood estimation or generalized likelihood ratio test viewpoints. The summation of the soft-thresholding transformation $(U_{\ell,k} - c)^+$ in (9) is more fundamental and can be interpreted from the following semi-Bayesian viewpoint. For a given candidate change-point ℓ , let Z_k be the indicator whether the k -th principal component is affected by the change in the out-of-control state or not, for $k = 1, \dots, d$. Assume that all principal components are independent, and each has a prior probability π getting affected by the changing event. That is, assume that the changing indicators Z_1, \dots, Z_d are iid with probability mass function $\mathbf{P}(Z_k = 1) = \pi = 1 - \mathbf{P}(Z_k = 0)$. When $Z_k = 1$, the k -th principal component is affected, and $U_{\ell,k}$ in (8) represents the evidence of possible change in the log-likelihood-ratio scale. Treating Z_k 's as the hidden states, and then the joint log-likelihood ratio statistic of Z_k 's and $X_{k,n}$ when testing $H_0 : Z_1 = \dots = Z_d = 0$ (no change) is

$$LLR(n) = \sum_{k=1}^d \{Z_k(\log \pi + U_{\ell,k}) + (1 - Z_k) \log(1 - \pi)\} - \sum_{k=1}^d \log(1 - \pi),$$

which becomes $\sum_{k=1}^d Z_k \{U_{\ell,k} - \log((1 - \pi)/\pi)\}$. Since the Z_k 's are unobservable, it is natural to maximize $LLR(n)$ over $Z_1, \dots, Z_d \in \{0, 1\}$. Hence, the generalized log-likelihood ratio becomes $\sum_{k=1}^d \max\{U_{\ell,k} - \log((1 - \pi)/\pi), 0\}$, which is exactly our test statistic Q_m in (9).

We should acknowledge that from the mathematical viewpoint, the multivariate functional PCA-based monitoring method in Paynabar et al. (2016) is the special case of Q_m in (9) when the soft-thresholding parameter $c = 0$, which is reasonable in that context because the number d of principal components is small (e.g., $d = 15$). However, our proposed method is a non-trivial extension of Paynabar et al. (2016) from the statistical or dimension reduction viewpoint: we consider a moderately large value d of principal components (e.g., $d = 45$), and a suitable choice of the soft-thresholding parameter $c > 0$ in (9) is essential to conduct another level of dimension reduction to smooth out those principal components that do not provide information of the change under the out-of-control state.

3.3 The Choices of Tuning Parameters

There are two tuning parameters in our proposed thresholded PCA methodology based on the test statistic Q_m in (9): one is the soft-thresholding parameter c in (9), and the other is the threshold L in (10). Practically, one needs to determine c first before selecting L , but below we will present the choice of L first for a given c since it is easier to understand from the statistical viewpoint.

In order to find the threshold L for our proposed methodology to satisfy the Type I error probability constraint, assume, for now, that the constant c in (9) is given. Then the constraint becomes $\mathbf{P}_{H_0}(Q_m > L) \leq \alpha$. Hence, the threshold L should be the upper α quantile of the distribution of Q_m in (9) for a given c under H_0 , which can be simulated by Monte Carlo method based on normal profiles and models, see Paynabar et al. (2016).

Let us now discuss the choice of soft-thresholding parameter c in (9). The baseline choice of c is $c_0 = 0$, which yields the approach of Paynabar et al. (2016) for the scenario when the number d of selected principal components is small. Intuitively, when the number d of principal components are large, the soft-thresholding parameter $c > 0$ in (9) should be large enough to filter out those non-changing bases $\hat{v}_k(t)$'s, but cannot be too large to

remove some changing principal components and lower the signal-to-noise ratios. Hence, a suitable choice of c will depend on the specific H_a and its effects on the basis projections.

Below we will discuss two different heuristic choices of the soft-thresholding parameter $c > 0$. For that purpose, by (9), we have

$$\mathbf{P}\left(\sum_{k=1}^d (U_{\ell,k} - c)^+ > L\right) \leq \mathbf{P}(Q_m > L) \leq \sum_{\ell=1}^{m-1} \mathbf{P}\left(\sum_{k=1}^d (U_{\ell,k} - c)^+ > L\right), \quad (12)$$

which becomes $(m-1)\mathbf{P}(\sum_{k=1}^d (U_{\ell,k} - c)^+ > L)$, as the data are iid over $\ell = 1, \dots, m-1$. Hence, from the asymptotic viewpoint, $\mathbf{P}(Q_m > L)$ and $\mathbf{P}(\sum_{k=1}^d (U_{\ell,k} - c)^+ > L)$ go to 0 at the same rate when m is fixed. In particular, when the Type I error constraint α goes to 0, the main probability of interest is to estimate $\mathbf{P}_{H_0}(\sum_{k=1}^d (U_{\ell,k} - c)^+ > L_c)$, where L_c is chosen so that this probably $\leq \alpha$. Our proposed choices of c correspond to two different methods to approximate the distribution of $\sum_{k=1}^d (U_{\ell,k} - c)^+$ under H_0 : one is the central limit theorem (CLT) when c is small, and the other is the extreme theorem when c is large. Since these two methods yield different results on c , we present them separately in Proposition 1, which assumes that χ_p^2 approximation applies to $U_{\ell,k}$'s.

Proposition 1. *Assume that $U_{\ell,k} \sim \chi_p^2$ under H_0 , for all $k = 1, \dots, d$;*

(a) *(The CLT approximation when c is small). Assume further that under H_a , exactly d_0 out of d principal components are affected in the sense that $U_{\ell,k} \sim \chi_p^2(\delta^2 p) = \boldsymbol{\epsilon}_{\ell k}^T \boldsymbol{\epsilon}_{\ell k}$ with $\boldsymbol{\epsilon}_{\ell k} \sim N(\delta, I_p)$ for $k = 1, \dots, d_0$, and $U_{\ell,k} \sim \chi_p^2$ for $k = d_0 + 1, \dots, d$. Then when both d_0 and $d - d_0$ are large, an appropriate choice of c is*

$$c_1 = \arg \min_{c \geq 0} \left\{ -\frac{(\mu_c^{(1)} - \mu_c)d_0}{\sqrt{d_0(\sigma_c^{(1)})^2 + (d - d_0)(\sigma_c)^2}} + \frac{\sqrt{d}\sigma_c}{\sqrt{d_0(\sigma_c^{(1)})^2 + (d - d_0)(\sigma_c)^2}} z_\alpha \right\}, \quad (13)$$

where $\mu_c = \mathbf{E}_0(U_{\ell,k} - c)^+$ and $\sigma_c = \text{Var}_0(U_{\ell,k} - c)^+$ when $U_{\ell,k} \sim \chi_p^2$; $\mu_c^{(1)} = \mathbf{E}_1(U_{\ell,k} - c)^+$ and $\sigma_c^{(1)} = \text{Var}_1(U_{\ell,k} - c)^+$ when $U_{\ell,k} \sim \chi_p^2(\delta^2 p)$.

(b) *(The extreme theory approximation when c is large). For fixed p channels, as $d \rightarrow \infty$, the soft-thresholding parameter c can be chosen as*

$$c_2 \approx p + 2 \log(d). \quad (14)$$

Proof: Due to page limit, let us only provide a sketch of the proof. In part (a), the c_1 value maximizes the power of the test under H_a subject to the Type I error constraint α , and the CLT is used to approximate error probabilities. That is the reason why we need some prior information on d_0 and δ under H_a . In our numerical studies, when such prior information of H_a is not available, our experiences suggest that $\delta = 1$ and $d_0 = d/3$ yield a good robust result under our simulation numerical setting.

The rationale of part (b) is completely different, and is similar to use the following well-known fact to choose the soft-thresholding parameter of $\sqrt{2 \log(d)}$ for d iid $N(0, 1)$ random variables, see Fan (1996),

$$\lim_{d \rightarrow \infty} \frac{\max_{1 \leq k \leq d} |Z_k|}{\sqrt{2 \log(d)}} = 1 \quad \text{almost surely}$$

when the Z_k 's are iid $N(0, 1)$. Here we extend the critical value from $\sqrt{2 \log(d)}$ for the $N(0, 1)$ -distributed Z_k 's to c_2 for the χ_p^2 -distributed $U_{\ell,k}$'s for fixed p as $d \rightarrow \infty$. These two critical values are asymptotically equivalent when $p = 1$, as $N(0, 1)^2$ is χ_p^2 -distributed with $p = 1$. To prove part (b) rigorously, we first use the fact

$$\mathbf{P}_{H_0} \left(\sum_{k=1}^d (U_{\ell,k} - c)^+ > L_c \right) < \mathbf{P}_{H_0} \left(\max_{1 \leq k \leq d} U_{\ell,k} > c \right) < \sum_{k=1}^d \mathbf{P}_{H_0} \left(U_{\ell,k} > c \right) = d \mathbf{P} \left(\chi_p^2 > c \right),$$

since we assume $U_{\ell,k} \sim \chi_p^2$ under H_0 . Next, we need use the asymptotic expression of $\mathbf{P}(\chi_p^2 > c)$ in Inglot and Ledwina (2006) to establish a useful lemma that $\log \mathbf{P}(\chi_p^2 > c) = -(c - p)/2 + O(\log c)$ for fixed p as $c \rightarrow \infty$. Then it is straightforward to prove part (b).

4 Case Study

In this section, we apply our proposed thresholded PCA method to the real forging manufacturing process dataset in Figures 1 and 2 in the Introduction. This dataset includes 207 normal profiles under the in-control state and 69 different fault profiles under the out-of-control state. It was analyzed in Paynabar et al. (2016) whose method can be thought of as the special case of our proposed method with the specific soft-thresholding parameter $c_0 = 0$. Below the choice of $c_0 = 0$ will be regarded as the baseline method, and we will focus on whether the values of c_1 and c_2 in Proposition 1 for the soft-thresholding parameter c in (9) can improve the performance or not as compared to the baseline value $c_0 = 0$.

First, we consider a specific case study setting in Paynabar et al. (2016) where 207 normal profiles are followed by the 69 fault profiles, i.e., the change-point $\tau = 207$ for the change-point model in (1), and the baseline method $c_0 = 0$ can successfully detect the true change-point. Our experiences show that our proposed method with either c_1 or c_2 can also correctly detect the change-point. In other words, if the change is significantly large, then all reasonable profile monitoring algorithms, including our proposed methods with any of the three c values in (9), will be able to detect the change correctly.

Below we will conduct extensive simulation studies that focus on detecting smaller changes. For better presentation, the remainder of this section is divided into two subsections. In subsection 4.1, we use the real profiles and B-splines to present the generative models of profiles under the in-control state and $2 \times 3 \times 7 = 42$ different out-of-control states. This allows us to generate observed profiles $\mathbf{X}_i(t)$'s from the change-point additive noise model in (1). In subsection 4.2, our proposed thresholded PCA methods are applied to the generated profiles $\mathbf{X}_i(t)$'s, and the performance of the values of c_1 and c_2 in Proposition 1 is then compared with that of the baseline value $c_0 = 0$.

4.1 Profile Generative Models

Let us provide a high-level description of our simulation setting. In each run of our simulation studies below, we generate $m = 200$ profiles from the change-point model in (1) with change-point $\tau = 100$, i.e., the first 100 profiles, $\mathbf{X}_1(t), \dots, \mathbf{X}_{100}(t)$, are generated from the in-control state, and the last 100 profiles, $\mathbf{X}_{101}(t), \dots, \mathbf{X}_{200}(t)$ are generated from one of the 42 out-of-control states. For each set of $m = 200$ simulated profiles, our proposed thresholded PCA method with three different soft-thresholding parameters c_0, c_1, c_2 , are applied to see whether they are able to correctly detect the change $\tau = 100$ or not. This process is repeated for 200 times, and the average performances are reported and compared for three different parameters c_0, c_1, c_2 . It is important to emphasize that the generative models below are only used to generate the $m = 200$ observable profiles $\mathbf{X}_i(t)$'s. Our proposed thresholded PCA methods are applied to those $m = 200$ profiles, and do not use any information or knowledge of these profile generative models.

For the generative models for profiles under the in-control state, we propose to build such a model by applying B-splines to the 207 normal profiles, $\mathbf{X}_1(t), \dots, \mathbf{X}_{207}(t)$, in the real forging dataset. To be more specific, we generate an unevenly spaced set of 66 B-spline basis in $[0, 1]$, and after orthogonalization and normalization we obtain basis $B_1(t), \dots, B_{66}(t)$ using the “orthogonalsplinebasis” Package in the free statistical software R 3.1.2. Based on our experiences, the choice of 66 basis yields the best tradeoff to balance the fitting of normal profiles and the computational simplicity, but it can easily be changed to another number. Then our proposed generative model for normal profiles is of the form

$$\mathbf{X}(t) = \sum_{i=1}^{66} \tilde{\boldsymbol{\theta}}_i B_i(t), \quad (15)$$

where the 4-dimensional vectors $\tilde{\boldsymbol{\theta}}_i$'s are assumed to be multivariate normally distributed with parameters estimated from the observed 207 normal profiles, see Figure 3.

For profiles under the out-of-control (OC) state, we assume that the generative OC model is the same as (15) but the means of $\tilde{\theta}_i$'s might change. We will consider a total of $2 \times 3 \times 7 = 42$ different OC cases, depending on three different factors. First, we consider two different scenarios, depending on how many components/channels of the 4-dimensional random vector $(\tilde{\theta}_i^{(1)}, \tilde{\theta}_i^{(2)}, \tilde{\theta}_i^{(3)}, \tilde{\theta}_i^{(4)})$ are involved with the change: (A) All 4 components/channels have new OC mean; and (B) Only the first 2 components/channels, $\tilde{\theta}_i^{(1)}$ and $\tilde{\theta}_i^{(2)}$ have OC mean (our proposed methods are not designed for Scenario B, and we run simulation to see their performance). Second, we consider three cases, depending on which subset of the 66 different $\tilde{\theta}_i$ in the model (15) changes their means, or equivalently, which location or interval of $[0, 1]$ changes at the original profile scale: (I) a local change for $30 \leq i \leq 37$; (II) a local change for $16 \leq i \leq 29$ and (III) a global change for all $1 \leq i \leq 66$. In the context of the original profiles, the locations of these three changes occur over intervals $\frac{200}{400} \leq t \leq \frac{300}{400}$, $\frac{99}{400} \leq t \leq \frac{149}{400}$ and $0 \leq t \leq 1$, respectively. Finally, we consider seven different magnitude values, so as to have reasonable detection powers regardless of the locations of the change. In particular, when the real-valued mean of $\tilde{\theta}_i^{(j)}$'s changes from θ_i to $\theta_i + 0.005 + 0.005 * \Delta$, we set $\Delta = h + 1$ for local change in Case (I), $\Delta = h$ for local change in Case (II), and $\Delta = 0.1 * h$ for global change in case (III). Here there are seven values of $h : h = 1, 2, \dots, 7$. Note that given the same magnitude of the change, it is the most difficult to detect the local change of Case (I) (where the peak of the profile occurs), and it is the easiest to detect the global change of Case (III). Here we assign different magnitudes so that the detection powers of these cases are comparable. In summary, there are $2 \times 3 \times 7 = 42$ OC cases depending on the channel, location, and magnitude of the changes, and all numerical values are inspired from the real forging dataset.

4.2 Performance Comparison

In this subsection, we report the performance of our proposed thresholded PCA method with three different choices of the soft-thresholding parameter c , and our objective is to see whether the c_1 and c_2 in Proposition 1 will yield a better performance as compared to the baseline $c_0 = 0$ in the sense of detecting those $2 \times 3 \times 7 = 42$ OC cases.

In order to have a fair comparison, we fix the number of principal components as $d = 45$ for all three choices of soft-thresholding c values, since on average that will explain more than 90% of the profiles variance. In addition, for each method, we choose the threshold L in (10) to satisfy Type I error constraint $\alpha = 0.05$. Also our proposed methods were developed under the assumption that all 4 components/channels are affected, and the magnitudes of the changes are unknown. Table 1 lists the specific values of c_0, c_1, c_2 used in our study. Note that the value of $c_0 = 0$ and c_2 do not depend on the location of the change, but the value of c_1 depends on the location of the change.

Figure 4 plots the detection power of our proposed methods with three different choices of soft-thresholding c values as functions of change magnitudes when all 4 components/channels of θ_i are actually changed simultaneously. The top panel deals with the OC-case (I) where a local change affects the rise, peak, and fall segments of the profiles, and all three methods seem to have comparable detection powers, although $c_0 = 0$ is slightly worse. The middle panel shows that under the OC case (II), both c_1 and c_2 can greatly improve the detection power as compared with the baseline $c_0 = 0$, especially when the change magnitude is small (e.g., $h \leq 5$). For large change magnitudes, all three methods have detection power close to 1, implying that all reasonable methods should be able to detect large changes.

A surprising observation of Figure 4 is the bottom panel that considers the OC case (III) when a global change occurs over $[0, 1]$. Intuitively, for a global change, one would expect that the change affects all principal components and hence thresholding might not help. However, the bottom panel of Figure 4 is counter-intuitive, as both c_1 and c_2 seem to

yield a larger detection power than $c_0 = 0$, especially for small magnitude h . To gain a deep understanding, Figure 5 plots the box plot of $U_{\ell=100,k}$ under the both IC and OC-case(III) states for all $d = 45$ principal components. From the box plots, for the global change, it is surprising that almost half of $U_{\ell,k}$'s have a similar or smaller median value under OC than IC. We feel that this is the reason why soft-thresholding help improve the detection power in the global change case, as it can filter out those $U_{\ell,k}$'s that have smaller OC values.

We also evaluate the performance of our proposed method in terms of estimating the change-point τ . When the true $\tau = 100$ is estimated as $\hat{\tau}$, we consider three different measures: $\mathbf{E}(|\hat{\tau} - \tau|)$, $P(|\tau - \hat{\tau}| \leq 1)$ (denoted by P1) and $P(|\tau - \hat{\tau}| \leq 3)$ (denoted by P3). Table 2 reports the Monte Carlo simulation results under these three criteria based on 200 runs. In general all three values c_0, c_1 and c_2 yield comparable results in terms of estimating τ , and it is interesting to note that the thresholding values c_1 and c_2 often have larger P1 and P3 than the baseline $c_0 = 0$ for the OC case (II) with the local-mean shift cases. This suggests that thresholding might be able to locate the small, local change more precisely. One “strange” observation in Table 2 is that $\mathbf{E}(|\hat{\tau} - \tau|)$ is not necessarily monotone as a function of the change magnitude h . We do not have a deep insight, and one possible explanation is because $|\hat{\tau} - \tau|$ takes on the integer values, $0, 1, 2, \dots, 100$, since both are integers.

Figure 6 plots the detection power of our proposed methods when only 2 out of 4 channels/components are affected. It is clear from the top and middle panels of Figure 6 that the c_1 and c_2 values greatly outperforms the baseline $c_0 = 0$ value for almost all shift magnitudes in the OC case of local changes. In the bottom panel for the OC case (III) of the global change, the detection power improvement is significant for c_2 as compared to the baseline $c_0 = 0$. We feel this might be due to the new spatial sparsity where the profile means of only two channels have shifted. While our proposed thresholded PCA method is not designed specifically for the spatial sparsity, the thresholding can actually take care

of spatial sparsity to yield better detection power. In addition, as compared to Figure 4, Figure 6 implies that the detection powers when only 2 out of 4 components have changed are less than those when all 4 components have changed.

5 Conclusion and Future Work

In this paper, we proposed a thresholded multivariate PCA for multichannel profile monitoring. Our proposed method essentially conducts dimension reduction in two steps: We first apply multivariate PCA to reduce high dimensional multichannel profiles to a reasonable number of features under the normal operational state, and then use soft-thresholding techniques to further select informative features under the out-of-control state. We also give several suggestions on how to select tuning parameters based on asymptotic analysis. Moreover, we used real forging process dataset and B-splines to build generative methods for multichannel profiles under the in-control state and $2 \times 3 \times 7 = 42$ different out-of-control states. Our numerical studies demonstrate that the soft-thresholding technique can significantly increase the detection power as compared to the baseline value $c_0 = 0$.

There are a number of interesting problems that have not been addressed here. From the theoretical point of view, it will be useful to investigate the efficiency of our proposed methods, and to find an optimal value of soft-thresholding parameter c that can adaptively adjust for different out-of-control states. Another direction is to investigate how to extend our proposed method to Phase II online profile monitoring. That will be more challenging, partly because it is more difficult to select informative principal components due to fewer out-of-control profiles since one observes profiles one at a time. Therefore, our research should be interpreted as a starting point for further investigation.

References

- Abdel-Salam, A. S. G., Birch, J. B., and Jensen, W. A. (2013). A semiparametric mixed model approach to phase i profile monitoring. *Quality and Reliability Engineering International*, 29(4):555–569.
- Berkes, I., Gabrys, R., Horváth, L., and Kokoszka, P. (2009). Detecting changes in the mean of functional observations. *Journal of the Royal Statistical Society: Series B (Statistical Methodology)*, 71(5):927–946.
- Chicken, E., Pignatiello Jr, J. J., and Simpson, J. R. (2009). Statistical process monitoring of nonlinear profiles using wavelets. *Journal of Quality Technology*, 41(2):198–212.
- Ding, Y., Zeng, L., and Zhou, S. (2006). Phase i analysis for monitoring nonlinear profiles in manufacturing processes. *Journal of Quality Technology*, 38(3):199–216.
- Fan, J. (1996). Test of significance based on wavelet thresholding and neyman’s truncation. *Journal of the American Statistical Association*, 91(434):674–688.
- Grasso, M., Colosimo, B., and Pacella, M. (2014). Profile monitoring via sensor fusion: the use of pca methods for multi-channel data. *International Journal of Production Research*, 52(20):6110–6135.
- Inglot, T. and Ledwina, T. (2006). Asymptotic optimality of new adaptive test in regression model. In *Annales de l’IHP Probabilités et statistiques*, volume 42, pages 579–590.
- Jensen, W. A., Birch, J. B., and Woodall, W. H. (2008). Monitoring correlation within linear profiles using mixed models. *Journal of Quality Technology*, 40(2):167–183.
- Jeong, M. K., Lu, J. C., and Wang, N. (2006). Wavelet-based spc procedure for complicated functional data. *International Journal of Production Research*, 44(4):729–744.

- Jeong, M. K., Lu, J. C., Zhou, W., and Ghosh, S. K. (2007). Data-reduction method for spatial data using a structured wavelet model. *International Journal of Production Research*, 45(10):2295–2311.
- Jin, J. and Shi, J. (2000). Diagnostic feature extraction from stamping tonnage signals based on design of experiments. *Journal of Manufacturing Science and Engineering*, 122(2):360–369.
- Noorossana, R., Saghaei, A., and Amiri, A. (2011). *Statistical Analysis of Profile Monitoring*, volume 865. New York: Wiley.
- Paynabar, K., Jin, J., and Pacella, M. (2013). Monitoring and diagnosis of multichannel nonlinear profile variations using uncorrelated multilinear principal component analysis. *IIE Transactions*, 45(11):1235–1247.
- Paynabar, K., Qiu, P., and Zou, C. (2016). A change point approach for phase-i analysis in multivariate profile monitoring and diagnosis. *Technometrics*, (forthcoming):1–37.
- Qiu, P. (2013). *Introduction To Statistical Process Control*. Chapman & Hall/CRC: Boca Raton, FL.
- Qiu, P., Zou, C., and Wang, Z. (2010). Nonparametric profile monitoring by mixed effects modeling. *Technometrics*, 52(3):265–277.
- Zou, C., Ning, X., and Tsung, F. (2012). Lasso-based multivariate linear profile monitoring. *Annals of Operations Research*, 192(1):3–19.

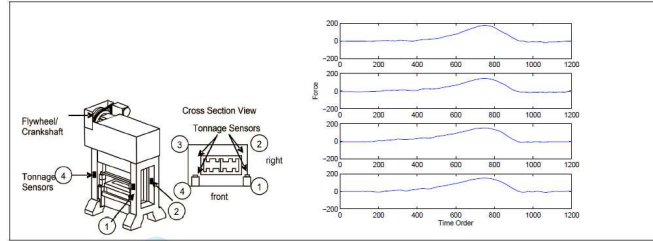


Figure 1: : *Left:* A forging machine with 4 tonnage sensors. *Right:* A single run sample of four-dimensional functional data.

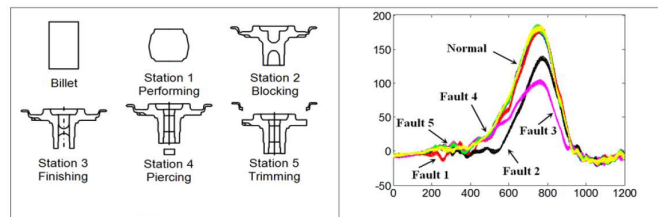


Figure 2: : *Left:* Shape of workpieces at each operation. *Right:* Tonnage profile for normal and missing operations.

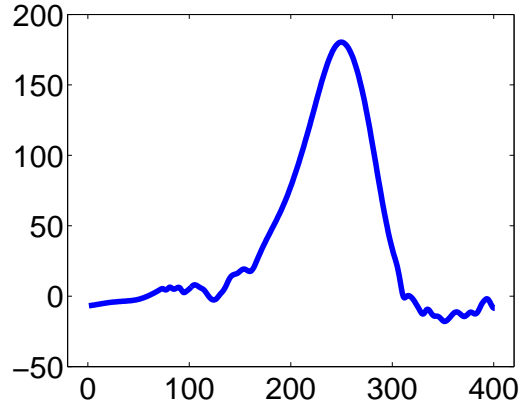


Figure 3: This figure plots the simulated in-control single profile $\mathbf{X}_m^{(1)}(t)$ based on an average of 200 replications. Interval $[0, 400]$ in the x-axis corresponds to $t \in [0/400, 400/400]$. This plot shows that the generative model in (15) under the in-control state indeed produced profiles that mimic the profiles from real forging process dataset in Figures 1 and 2.

Table 1: The value of d_0 and soft-thresholding parameters c 's

	c_0	d_0	c_1	c_2
OC-case (I)	0	15	4.9	11.6
OC-case (II)	0	9	7.0	11.6
OC-case (III)	0	12	4.5	11.6

Note: All our proposed methods were developed under the assumption that all 4 components/channels are affected, and the magnitudes of the changes are unknown. Table 1 lists the specific values of c_0, c_1, c_2 used in our study. Note that the value of $c_0 = 0$ and c_2 do not depend on the location of the change, but the value of c_1 depends on the location of the change.

Note that when computing the c_1 value in Proposition 1, we need to know the value of d_0 , the number of affected principal components that are relevant to the change among a total of $d = 45$ principal components. Here the value d_0 is chosen by the following data-driven method: We first obtain $U_{\ell,k}^{H_0}\{k = 1, \dots, d\}$'s under H_0 using the simulated in-control profiles and record the value A as the top 10% value of $U_{\ell,k}^{H_0}$'s. Then, we compute $U_{\ell,k}^{H_1}\{k = 1, \dots, d\}$'s under H_1 using simulated out-of-control profiles, and count how many $U_{\ell,k}^{H_1}$'s are greater than such threshold A . This gives an estimate of d_0 since it indicates the number of altered $U_{\ell,k}$'s if a specific fault occurs. For the purpose of easy computation and comparison, the out-of-control scenario was conducted when all 4 components of affected θ_i are changed, and the same d_0 and c_1 values were used in the scenario when only 2 out of 4 components are changed.

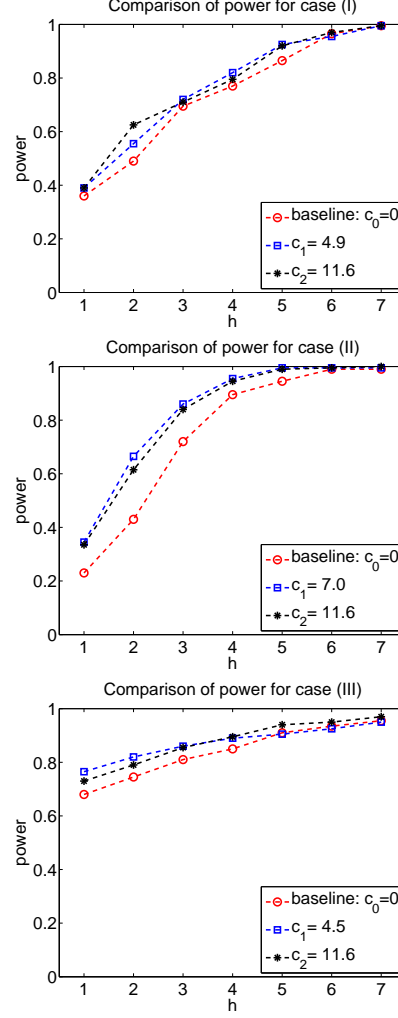


Figure 4: When all 4 channels/components are affected. The three plots correspond to three OC cases, depending on which subset of the 66 different $\tilde{\theta}_i$ in the model (15) changes their means. *Upper*: case (I) with a local change for $30 \leq i \leq 37$; *Medium*: case (II) with a local change for $16 \leq i \leq 29$ and *Bottom*: case (III) with a global change for all $1 \leq i \leq 66$. In each figure, each curve represents our proposed method with a specific soft-thresholding c values: Red line with circle (c_0); blue line with square (c_1); and black line with star (c_2). The detection power of each method is plotted as the function of the 7 different change magnitudes.

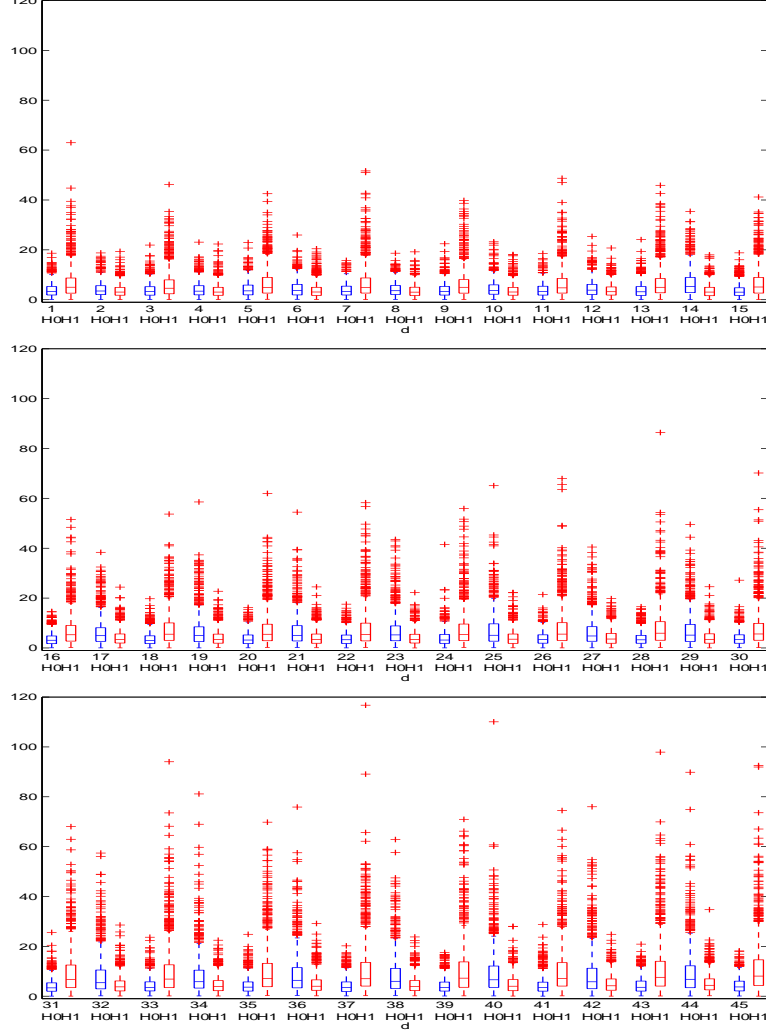


Figure 5: Box plots of $U_{\ell=\tau=100,k}$ under the H_0 hypothesis and H_1 hypothesis for case (III) under all 4 channels affected scenario with $h = 4$ based on 1000 replications. X axis with $k = 1, \dots, 45$ represents the projection on the k 'th principal components. This plot implies that even for the global change, the OC distribution of the $U_{\ell,k}$'s is not necessarily stochastically larger than those IC distribution over all $k = 1, \dots, 45$ principal components. We feel that this is the reason why soft-thresholding can improve the detection power in the global change case, as it can filter out those $U_{\ell,k}$'s that have smaller OC values.

Table 2: Comparison of detection biases for each algorithms under 3 different out-of-control cases for all 4 channels affected scenario.

		$\mathbf{E}(\hat{\tau} - \tau)$			$\mathbf{P}(\tau - \hat{\tau} \leq 1)$			$\mathbf{P}(\tau - \hat{\tau} \leq 3)$		
	h	c_0	c_1	c_2	c_0	c_1	c_2	c_0	c_1	c_2
Case (I)	1	5.18 ± 1.71	1.14 ± 1.89	0.86 ± 2.09	0.18	0.15	0.19	0.40	0.44	0.36
	2	1.57 ± 1.33	1.89 ± 1.35	2.65 ± 1.73	0.22	0.22	0.22	0.51	0.50	0.39
	3	0.95 ± 1.21	1.51 ± 1.27	0.59 ± 1.38	0.27	0.26	0.25	0.54	0.54	0.47
	4	0.81 ± 1.10	1.03 ± 1.02	0.59 ± 1.26	0.31	0.36	0.33	0.57	0.63	0.54
	5	0.28 ± 0.86	0.30 ± 0.88	0.09 ± 0.77	0.38	0.36	0.42	0.63	0.63	0.63
	6	0.13 ± 0.73	0.13 ± 0.79	0.58 ± 0.47	0.41	0.42	0.46	0.65	0.68	0.66
	7	0.14 ± 0.54	0.63 ± 0.46	0.29 ± 0.49	0.47	0.46	0.49	0.70	0.72	0.70
Case (II)	1	2.15 ± 2.37	0.16 ± 2.45	2.30 ± 2.30	0.09	0.22	0.22	0.24	0.36	0.36
	2	1.98 ± 1.64	0.78 ± 1.57	0.18 ± 1.50	0.24	0.35	0.35	0.48	0.51	0.53
	3	1.12 ± 0.88	0.76 ± 1.08	1.19 ± 1.23	0.39	0.40	0.42	0.60	0.61	0.63
	4	0.11 ± 0.70	0.67 ± 0.78	0.43 ± 0.71	0.48	0.53	0.56	0.72	0.76	0.76
	5	0.51 ± 0.62	0.02 ± 0.54	0.24 ± 0.57	0.58	0.67	0.65	0.78	0.83	0.86
	6	0.22 ± 0.53	0.51 ± 0.49	0.49 ± 0.49	0.70	0.76	0.73	0.86	0.91	0.90
	7	0.50 ± 0.48	0.02 ± 0.14	0.07 ± 0.16	0.77	0.81	0.80	0.90	0.95	0.95
Case (III)	1	0.07 ± 1.13	0.16 ± 1.07	1.18 ± 1.25	0.35	0.34	0.31	0.57	0.57	0.50
	2	0.58 ± 1.11	0.37 ± 1.01	0.52 ± 1.07	0.39	0.35	0.34	0.60	0.61	0.54
	3	0.85 ± 1.05	0.67 ± 0.94	0.51 ± 0.84	0.43	0.39	0.38	0.64	0.61	0.56
	4	0.15 ± 0.90	0.11 ± 0.73	0.43 ± 0.82	0.45	0.41	0.40	0.67	0.64	0.61
	5	0.13 ± 0.84	0.11 ± 0.66	0.27 ± 0.55	0.47	0.45	0.45	0.69	0.68	0.66
	6	0.44 ± 0.79	0.04 ± 0.58	0.03 ± 0.52	0.49	0.48	0.46	0.70	0.71	0.67
	7	0.39 ± 0.63	0.15 ± 0.54	0.01 ± 0.53	0.51	0.49	0.47	0.72	0.72	0.67

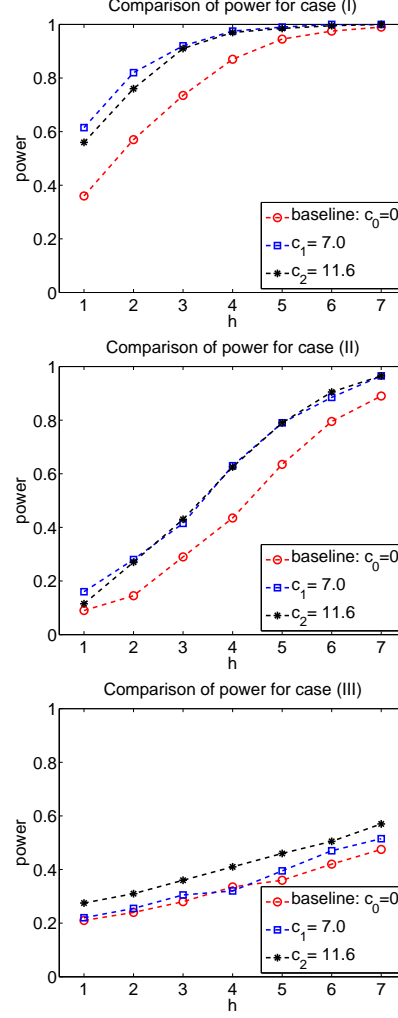


Figure 6: When only 2 out of 4 channels/components are affected. The three plots correspond to three OC cases, depending on which subset of the 66 different $\tilde{\theta}_i$ in the model (15) changes their means. *Upper:* case (I) with a local change for $30 \leq i \leq 37$; *Medium:* case (II) with a local change for $16 \leq i \leq 29$ and *Bottom:* case (III) with a global change for all $1 \leq i \leq 66$. In each figure, each curve represents our proposed method with a specific soft-thresholding c values: Red line with circle (c_0); blue line with square (c_1); and black line with star (c_2). The detection power of each method is plotted as the function of the 7 different change magnitudes.